

Ante Bing, Yuchen Hu, Melanie Prague, Alison L. Hill, Jonathan Z. Li, Ronald J. Bosch,  
Victor DeGruttola and Rui Wang\*

# Comparison of empirical and dynamic models for HIV viral load rebound after treatment interruption

<https://doi.org/10.1515/scid-2019-0021>

Received November 15, 2019; accepted June 30, 2020; published online August 17, 2020

## Abstract

**Objective:** To compare empirical and mechanistic modeling approaches for describing HIV-1 RNA viral load trajectories after antiretroviral treatment interruption and for identifying factors that predict features of viral rebound process.

**Methods:** We apply and compare two modeling approaches in analysis of data from 346 participants in six AIDS Clinical Trial Group studies. From each separate analysis, we identify predictors for viral set points and delay in rebound. Our empirical model postulates a parametric functional form whose parameters represent different features of the viral rebound process, such as rate of rise and viral load set point. The viral dynamics model augments standard HIV dynamics models—a class of mathematical models based on differential equations describing biological mechanisms—by including reactivation of latently infected cells and adaptive immune response. We use Monolix, which makes use of a Stochastic Approximation of the Expectation–Maximization algorithm, to fit non-linear mixed effects models incorporating observations that were below the assay limit of quantification.

**Results:** Among the 346 participants, the median age at treatment interruption was 42. Ninety-three percent of participants were male and sixty-five percent, white non-Hispanic. Both models provided a reasonable fit to the data and can accommodate atypical viral load trajectories. The median set points obtained from two approaches were similar:  $4.44 \log_{10}$  copies/mL from the empirical model and  $4.59 \log_{10}$  copies/mL from the viral dynamics model. Both models revealed that higher nadir CD4 cell counts and ART initiation during acute/recent phase were associated with lower viral set points and identified receiving a non-nucleoside reverse transcriptase inhibitor (NNRTI)-based pre-ATI regimen as a predictor for a delay in rebound.

**Conclusion:** Although based on different sets of assumptions, both models lead to similar conclusions regarding features of viral rebound process.

---

Bing and Hu contributed equally to this work.

---

\*Corresponding author: Rui Wang, Department of Population Medicine, Harvard Pilgrim Health Care Institute and Harvard Medical School and Department of Biostatistics, Harvard T. H. Chan School of Public Health, Boston, MA, 02215, USA,  
E-mail: rwang@hsph.harvard.edu. <https://orcid.org/0000-0001-5007-193X>

Ante Bing, Department of Mathematics and Statistics, Boston University, Boston, MA, 02215, USA

Yuchen Hu, Department of Population Medicine, Harvard Pilgrim Health Care Institute and Harvard Medical School, Boston, MA, 02215, USA; Department of Biostatistics, Harvard T. H. Chan School of Public Health, Boston, MA, 02215, USA

Melanie Prague, University of Bordeaux, Inria Bordeaux Sud-Ouest, Inserm, Bordeaux Population Health Research Center, SISTM Team, UMR 1219, F-33000 Bordeaux, France

Alison L. Hill, Program for Evolutionary Dynamics, Harvard University, Cambridge, MA, 02138, USA

Jonathan Z. Li, Brigham and Women's Hospital, Harvard Medical School, Boston, MA, 02215, USA

Ronald J. Bosch and Victor DeGruttola, Department of Biostatistics, Harvard T. H. Chan School of Public Health, Boston, MA, 02215, USA

**Keywords:** dynamic system; empirical; predictors; treatment interruption; viral rebound.

## 1 Introduction

Although antiretroviral therapy (ART) suppresses HIV replication thereby slowing disease progression, it cannot eradicate the infection. Even among those with suppressed virus, latent HIV reservoirs exist as replication-competent proviruses integrated into human DNA of infected cells; these reservoirs can induce viral rebound when ART is discontinued (Vanhamel, Bruggemans, and Debyser 2019). HIV-1 RNA viral load (VL) measures the amount of virus released from infected cells into the blood plasma and provides essential information about disease progression (Dybul et al. 2002; Mellors et al. 1997). After ART discontinuation, viral load usually increases sharply to a peak within 10 weeks, followed by a decrease to a level that is somewhat stable over a timescale of months; this level is often referred to as a set point. Characterizing features of the viral rebound trajectories (such as the delay in rebound and the set point) and identifying host, virological, and immunological factors that are predictive of these features are central to HIV cure research (Julg et al. 2019).

A variety of empirical and dynamic modeling approaches have been proposed to characterize viral load trajectories in primary infection and after treatment initiation (Wu 2009). These models often provide both biological interpretability and mathematical simplicity. For example, Wu and Ding (1999) showed that a simple bi-exponential nonlinear mixed effects model (NLME) can be used to model viral decay process in the first and second phases after ART initiation. Wu and Zhang (2002) extended the bi-exponential model to a semi-parametric NLME model, where the second-phase viral decay rate was modeled by a time-dependent smooth curve instead of a constant value. Fitzgerald, DeGruttola, and Vaida (2002) proposed a two-component NLME model for the trajectory of HIV-1 RNA until rebound, in which one component models the second-phase decay process and the other component reflects the development of viral resistance to treatment with possible viral rebounds. These models were developed with non-linear functional forms to describe variable rates of decline or decline followed by viral rebound while on potentially failing antiretroviral treatment. Vaida and Liu (2009) used a four-parameter logistic functional form to model viral load trajectories for acutely infected subjects. Moulton, Curriero, and Barroso (2002) proposed a Bernoulli/log-gamma mixture model with shared parameters to investigate the effects of an antiretroviral therapy regimen on HIV-1 shedding in the seminal fluid.

In addition to modeling the non-linear trajectory with a specific parametric functional form, such a trajectory can be accommodated by incorporating pre-specified change points in linear models (Thiébaut et al. 2005) as well as the use of cubic B-splines in regression models (Brown, Ibrahim, and DeGruttola 2005) and of penalized spline approaches (Liang and Xiao 2006; Zhao et al. 2020). These methods require specification of the change points or selection of knots, although the penalized spline approach is less sensitive to the number and location of knots compared to the regression spline approach.

Methods to fit linear and nonlinear mixed effects models that relax the normality assumptions on the random errors and random-effects (Huang and Dagne 2010, 2012; Lachos, Bandyopadhyay, and Dey 2011; Matos et al. 2013; Garay et al. 2017), and/or account for the left-censoring of viral load values due to the lower limit of assay quantification (Dagne 2016; Lachos et al. 2015; Lavielle 2014; Vaida and Liu, 2009; Vaida, Fitzgerald, and DeGruttola 2007; Wang et al. 2020) have been investigated. Here, we consider a parametric model with a flexible functional form that mimics the shape of observed viral rebound trajectories after treatment interruption and is also intended to provide biological insights (Wang et al. 2020). Key features of viral rebound trajectories such as the viral load set points and rates of rise are represented by parameters in the model.

Mechanistic mathematical models, represented as systems of non-linear ordinary differential equations (ODEs), are well-established tools to describe the dynamics of HIV infection. Earlier pioneering work by Ho et al. (1995), Wei et al. (1995), and Perelson et al. (1997) lead to the development

of the basic model of “viral dynamics”, and much subsequent work has focused on including additional interactions, such as antiviral immune responses (see Nowak and May (2000); Perelson and Ribeiro (2013); Schwartz et al. (2016); Perelson and Ribeiro (2013) for a review). In these models, the parameters represent quantities with clear biological meaning – such as the rate of clearance of free virus from the plasma or the number of virions released from an infected cell – some of which can be estimated directly from experiments (Chen et al. 2007; Ramratnam et al. 1999), but others are very difficult to measure directly (such as *in vivo* viral fitness or the lifespan of infected cells). By fitting these models to viral load trajectories, the goal is to estimate the values of these parameters and hence gain quantitative insights into the dynamics and pathogenesis of HIV. While most model-fitting has focused on the viral dynamics after treatment initiation (Drylewicz, Commenges, and Thiebaut 2012; Markowitz et al. 2003; Prague et al. 2012), there has been a recent surge of interest in the dynamics of viral rebound after treatment interruption. Many of these investigations have focused on estimating the rate of reactivation of the latently infected cells that kick-start viral rebound (Borducchi et al. 2018; Conway and Perelson 2015; Hill et al. 2016; Pinkevych et al. 2015; Rong and Perelson 2009).

In this paper, we use a model of viral dynamics that is augmented to include antiviral immune responses and reactivation of latently infected cells (Prague et al. 2019). Although this model is implemented as a deterministic system of ODEs, its structure is such that it mimics the dynamics of stochastic and variable delays until reactivation of virus from latency. Both identifiability of, and inference on, model parameters for such complex nonlinear models are known to be challenging. To account for within- and between-individual variations in the model parameters, methods have been developed to use statistical random effects models in conjunction with non-linear ODE dynamical systems. Early work includes Putter et al. (2002); Huang, Liu, and Wu (2006); Samson, Lavielle, and Mentré (2006), and Guedj et al. (2007) among others, and more recent work include Prague et al. (2013); Wang et al. (2014), and Liu et al. (2019).

The aim of this paper is to investigate and compare the two aforementioned modeling strategies, parametric nonlinear mixed effect modeling and mechanistic mathematical modeling, for characterizing the HIV viral load rebound process after treatment discontinuation. These models can also aid in identifying biomarkers that predict features of this process. Section 2 introduces the notation and formulation of these models and describes the fitting procedures. Section 3 describes the dataset from six AIDS Clinical Trial (ACTG) analytic treatment interruption (ATI) studies used in our analyses and presents results from fitting the models to these data. We compare the models using the Akaike Information Criteria (AIC), the Bayesian Information Criteria (BIC), and the corrected Bayesian Information Criteria (BICc). We also use graphical display to compare the goodness of fits for the two models. In addition, we use both models to identify pre-ATI predictors for features of the viral rebound process. We conclude the paper with a discussion in Section 4.

## 2 Modeling the viral load trajectory

### 2.1 Notation

Let  $y_{ij}$  be the log10-transformed HIV viral load of the  $i$ th subject at  $j$ th time point after treatment interruption,  $t_{ij}$  be the corresponding time point, where  $i=1, 2, \dots, n$  and  $j=1, 2, \dots, n_i$ . We investigate two models that characterize trajectories of  $y_{ij}$  over time.

### 2.2 A parametric nonlinear mixed effect model

Parametric nonlinear mixed effect models for HIV viral load dynamics are an active area of research. Wang et al. (2020) proposed a nonlinear mixed effect model that can capture the HIV viral load dynamics after treatment interruption for both viral rise to a peak value and viral decay phase to a fairly stable value (referred

to as set point). Individual trajectories can be estimated by incorporating random effects on model parameters. Specifically, the model is:

$$y_{ij} = h(\beta_i, t_{ij}) + \varepsilon_{ij}, \varepsilon_{ij} \sim N(0, \sigma^2)$$

$$h(\beta_i, t) = \beta_{1i} \frac{t}{t + e^{\beta_2 i - \beta_3 i t}} + \beta_{4i} \frac{1}{1 + e^{\beta_5 i t}}$$

Here  $\beta_{ki} = \beta_k + \tau_{ki}$ ,  $k=1,2,3,4,5$ , where the random effects  $\tau_i = (\tau_{1i}, \tau_{2i}, \tau_{3i}, \tau_{4i}, \tau_{5i})^T$  are assumed to follow a multivariate normal distribution  $\tau_i \sim N(0, G)$  for some positive definite matrix  $G$ . The random effects  $\tau_i$  are assumed to be independent of the errors  $\varepsilon_{ij}$ . We use  $\beta$  to denote the vector consisting of  $\beta_k$ ,  $k=1, \dots, 5$ .

This choice of model takes into consideration the biological interpretability of parameters. The functional form, shown above, includes a specific parameter ( $\beta_1$ ) to represent viral set point, the level at which virus tends to be stable over time. Delay in rise and rate of rise are characterized by  $\beta_2$  and  $\beta_3$ , respectively.  $\beta_4/2$  represents the starting value, and  $\beta_5$ , the rate of decline from the peak. The proposed model allows direct assessment of covariate effects on parameters of interest (e.g., those that characterize viral set point). In Section 3, we estimate the covariate effects on various parameters of this model to identify pre-ATI predictors for features of viral rebound process.

### 2.3 A viral dynamics model

As mentioned above, mechanistic models, often formulated as systems of ordinary differential equations (ODEs), have been used to model HIV viral load trajectories after ART initiation (Wu 2005). Mechanistic models have the advantage of being able to incorporate scientific knowledge regarding mechanisms – in our setting, this knowledge includes the interactions of HIV viral particles and immune cells. For our analyses, we use a version of the viral dynamics model that allows for the presence of latently infected cells and immune responses to HIV antigens. The refined model is flexible enough to describe two different possible patterns of rebound kinetics depending on the size and reactivation rate of the latent reservoir: (1) latent cells reactivate frequently and rebound occurs rapidly, and (2) reactivation from latency is rare and the delay until the first lineage arises from the latent cells is variable. Previously proposed viral dynamics models do not account for pattern (2) and might therefore lead to underestimation of the reservoir reactivation rate. This model has been shown to perform well in fitting HIV/SIV rebound data (Prague et al. 2019).

This five-dimensional ODE system includes the following variables: uninfected cells ( $T$ ), infected cells ( $I$ ), effector immune cells ( $E$ ), free virus ( $V$ ) and precursor immune cells ( $P$ ). It is described by the following set of equations:

$$\begin{aligned}\dot{T} &= \lambda - \beta TV - d_T T \\ \dot{I} &= \alpha + \frac{\beta TV}{1 + (E/N_E)} - d_I I \\ \dot{V} &= kI - cV \\ \dot{P} &= m + p(1-f) \frac{V}{V + N_P} P - d_P P \\ \dot{E} &= pf \frac{V}{V + N_P} P - d_E E\end{aligned}$$

As depicted in Figure 1C, uninfected target cells  $T$  are produced at a constant rate  $\lambda$  and die at rate  $d_T$ . Free viruses  $V$ , cleared at rate  $c$ , enter target cells  $T$  at infection rate  $\beta$  and produce infected cells  $I$ , which release free viruses at rate  $k$ . The precursor immune cells are produced at a constant rate  $m$  and die at rate  $d_P$ . They encounter viral antigen, proliferate at rate  $pV/(V + N_P)$  and produce effector immune cells  $E$ . A fraction  $f$  of precursor cells revert to the precursor state. During viral rebound,  $m$  primarily represent reactivation of memory cells. Effector cells reduce the rate of infection to  $\beta/(1 + E/N_E)$ . Latently infected cells reactivate at rate

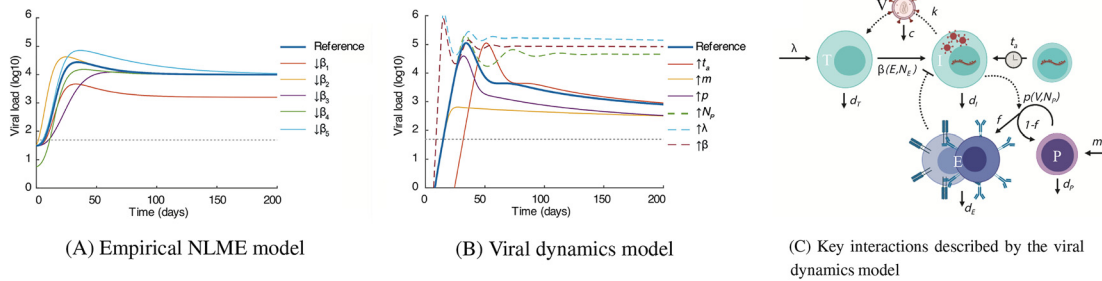


**Figure 1:** Summary of both the empirical and viral dynamics model. In (A) and (B) below, the effect of each individual parameter is demonstrated by changing only that parameter compared to a reference case. (A) Time course of viral load simulated by the empirical model. Parameters: for reference (and fold-change),  $\beta_1 = 4.0$  (0.8),  $\beta_2 = 3.0$  (0.5),  $\beta_3 = 1.0$  (0.5),  $\beta_4 = 3.0$  (0.5),  $\beta_5 = 0.3$  (0.5). (B) Time course of viral load simulated by the viral dynamics model. Parameters: for baseline (and fold-change),  $t_a = 0.01$  (100),  $m = 1.0$  (100),  $p = 1.0$  (2),  $N_p = 10^6$  (100),  $\lambda = 300$  (2),  $\beta = 6e-7$  (2). For the  $\lambda$  and  $\beta$  curves, the reference case is that of higher  $N_p$ , since only when there is a weak immune response (high  $N_p$ ) do  $\lambda$  and  $\beta$  impact the set point and peak. Other parameters are fixed at values used in model fitting. Note that the units that go into the model are viral load (copies/mL) and time (days) for the viral dynamics model but log10 viral load and time (weeks) for the empirical model. (C) Diagram of the key interactions described by the viral dynamics model. The model tracks the reactivation of latently infected cells, the spread of virus between target cells, and an antiviral immune response that limits infection. Details provided in the text.

$a$ , or expressed another way, every  $t_a$  days on average. When latent cell activation is rare, there can be long wait times until the first cell reactivates. The mathematical relationship between the fitted parameter  $t_a$  and the effective reactivation rate  $a$  in the ODE is described in detail in Prague et al. (2019).

To achieve parameter identifiability, a subset of parameters are assumed to be known and set to fixed values. Prague et al. (2019) provided a detailed identifiability analysis for this model, where they used the method of invariance to scaling transformations described in Castro and de Boer (2020) to examine the identifiability of the model parameters based on viral load data only. These results were further confirmed using methods based on differential algebra (Bellu et al. 2007) and exact arithmetic rank (Karlsson, Anguelova, and Jirstrand 2012). In summary, nearly all of the parameters are theoretically identifiable, except that one parameter from each of the sets  $\{\lambda, a, k\}$  and  $\{N_E, m\}$  is always non-identifiable. This motivates the decision to fix  $k$  and  $N_E$ . However, despite the theoretical identifiability, the simulation studies in Prague et al. (2019) revealed the difficulty in identifying these parameters in practice. Therefore, the values of  $f$ ,  $c$ ,  $d_T$ ,  $d_I$ ,  $d_E$ , and  $d_P$  are fixed using previously reported experimental estimates as in Prague et al. (2019). The parameters that remain to be estimated are:  $\lambda$ ,  $m$ ,  $p$ ,  $N_p$ ,  $t_a$ , and  $\beta$ . In Section 3, we assess covariate effects on different aspects of viral dynamics and rebound trajectories.

## 2.4 Model fitting

Both models are fit using Monolix, which makes use of a Stochastic Approximation of the Expectation–Maximization algorithm (Samson, Lavielle, and Mentré 2006) with random effects included on all parameters. The viral load values below level of quantification and the random effects are treated as missing data. At each iteration, the missing data are imputed using Gibbs sampling. The random effects are sampled from their conditional distribution conditional on observed data, imputed censored observations, and current parameter values, using a Metropolis–Hastings algorithm as outlined in Comets, Lavenu, and Lavielle 2011. The unobserved censored (i.e., below assay limit) observations are imputed from their conditional distribution conditional on observed data, sampled random effects, and current parameters. Note that conditional on the random effects, the unobserved censored observations from the same individual are independent; hence, they can be imputed separately from a truncated normal distribution. This imputation strategy is then used multiple times to approximate the conditional expectation of the log-likelihood for the subsequent maximization step. The

standard error is calculated using the Fisher information matrix corresponding to the observed likelihood, obtained by stochastic approximation (Comets, Lavenu, and Lavielle 2011).

We evaluate the effect of pre-ATI predictors on delay in rebound and viral set points. For the empirical NLME model, delay in rebound is captured by parameter  $\beta_2$  and the viral set point is represented by parameter  $\beta_1$ . For the viral dynamics model, delay in rebound is characterized by  $t_a$ . Although the viral set point is not a parameter in the viral dynamics model, it can be obtained by finding the equilibrium of the dynamical system for which viral load is non-zero. We used the rootSolve package in R to solve for viral set points. Covariate effects on  $\beta_1$ ,  $\beta_2$ , and  $t_a$  are assessed by adding a term for each covariate, the product of a fixed-effect parameter and the covariate, to these parameters and fitting the model. This allows for estimation of model parameters including covariate effects in a single step. For estimation of the covariate effect on viral set points for the viral dynamics model, we use a two-step procedure: (1) calculate these set points from the model, and (2) fit a least squares regression model of the set points on the covariates.

## 3 Results based on six ACTG studies

### 3.1 Data source

We obtained data from six ACTG studies: 371 (Volberding et al. 2009), A5024 (Kilby et al. 2006), A5068 (Jacobson et al. 2006), A5130 (Gandhi et al. 2009), A5187 (Rosenberg et al. 2010), A5197 (Schooley et al. 2010), in total of 346 participants. These participants were on suppressive ART for various amount of time and all participants had suppressed viral load (e.g., <50 copies/mL) at the start of treatment interruption.

The measurement times varied 0 to 225 weeks after treatment interruption; 74.5% of measurements were collected before week 24 after treatment interruption. As our main interest lies in the time period before participants achieve set point and as most do so before 24 weeks, we restrict our analyses to the first 24 weeks following ART discontinuation. Studies 371, A5024, A5068, A5130, A5187, A5197 contribute 15.8, 17.9, 26.2, 9.1, 5.6, 25.4% of measurements, respectively. For participants of ACTG 371, A5024, A5068, and A5197, viral loads were typically measured weekly or biweekly until week 12, then every 4 weeks thereafter. A5187 participants had viral loads measured biweekly up to week 22; A5130 participants were measured weekly up to week 12, then biweekly until week 20, and every 4 weeks thereafter.

Among the 346 participants, the median age at treatment interruption was 42 and the 25 and 75% quantiles were 37 and 47. 93% of participants were male and 65%, white non-Hispanic. Table 1 presents descriptive statistics for the participant population. In the combined dataset, 22.9% viral load measurements were censored at the lower limit of assay quantification, which was 50 copies/mL in these studies. Most participants (89.9%) had censored observations before or on week 3; only 5.5% had censored observations after week 10.

ACTG 371 tested the hypothesis that ART in early HIV infection achieves better viral control in acute compared to recent infection 24 weeks after treatment interruption (Volberding et al. 2009). Except for 371, participants in the other five studies were randomized to various immune-stimulating interventions or placebo prior to ART interruption (see Table 1). No intervention was given to participants after treatment interruption.

### 3.2 Model fitting results

Figure 2 presents the individual data trajectories for all 346 individuals (panel (A)) and fitted curves for a randomly selected nine individuals using the two modeling approaches (panel (B)). The point estimate and the 95% confidence interval estimates for the fixed effects parameters are provided in Table 2. The estimated viral load set point  $\beta_1$  was  $3.61 \log_{10}$  copies/mL from the empirical NLME model. For the viral dynamics model, the estimated target cell input rate  $\lambda$  was 494 (cells/ mL-day), and the estimated viral infectivity rate,  $\beta$ ,  $3.72 \times 10^{-7}$  (mL/copies-day). The estimated time between latent cell reactivations,  $t_a$ , and the immune memory input rate,  $m$ , were 0.03 (days) and 67.9 (cells/mL-day) respectively. Maximal immune proliferation rate  $p$  was 5.57/day.

**Table 1:** Participant Characteristics (n=346).

Characteristics	Mean (SD)
	n (%)
Age at ATI	42 (8.3)
ART duration, years	5 (3.6)
Sex	
Male	322 (93%)
Infection phase at ART initiation	
Acute	37 (10.7%)
Recent	54 (15.6%)
Chronic	255 (73.7%)
NNRTI-based regimen	
Yes	158 (45.7%)
Nadir CD4 (cells/mm <sup>3</sup> )	
≤200	38 (11.0%)
201–500	188 (54.3%)
501+	120 (26.6%)
Missing	28 (8.1%)
Immune-stimulating intervention received prior to ATI	
A5024	
ALVAC-HIV (vCP1452)	17 (34%)
IL2 + ALVAC-HIV (vCP1452)	11 (22%)
IL2 + placebo ALVAC	10 (20%)
Placebo ALVAC	12 (24%)
A5068	
ALVAC-HIV (vCP1452)	19 (26.8%)
ALVAC-HIV (vCP1452) + short-term ART withdraw	13 (18.3%)
Placebo ALVAC	20 (28.2%)
Placebo ALVAC + short-term ART withdrawals	19 (26.8%)
A5130	
ALVAC-HIV (vCP1452) + KLH	15 (53.6%)
DCs infected w/ ALVAC-HIV (vCP1452) + KLH	13 (46.4%)
A5187	
VRC-HIVDNA009-00-VP	10 (50%)
Placebo VRC-HIVDNA009-00-VP	10 (50%)
A5197	
MRK Ad5 HIV-1 gag	73 (68.9%)
Placebo MRK Ad5 HIV-1 gag	33 (31.1%)

Finally, the half-maximally stimulating level of virus  $N_p$  was  $40.4 \times 10^5$  (copies/mL). The model fitting statistics AIC, BIC, and BICc were similar from the two models (Table 3).

Individual fitted curves are generally close to the observed data (Figure 2B). We plotted the censored observations as triangles at the assay limit of quantification (i.e., 50 copies/mL). As expected, the predicted values for those observations (represented by triangles from both models) were generally lower than the assay limit. The fitted curves from the NLME model were smoother than those from the viral dynamics model, reflecting the assumed smooth parametric form in the empirical NLME model. Both models can accommodate atypical viral load trajectories (see for example Patient ID: 40 from Figure 2). We also examined the observed and predicted values using individual parameters and histograms of the individual weighted residuals from the two models (see Figure 3). The patterns were very similar, suggesting that both models provided a reasonable fit to the data. We performed sensitivity analyses by assuming a lognormal distribution for the

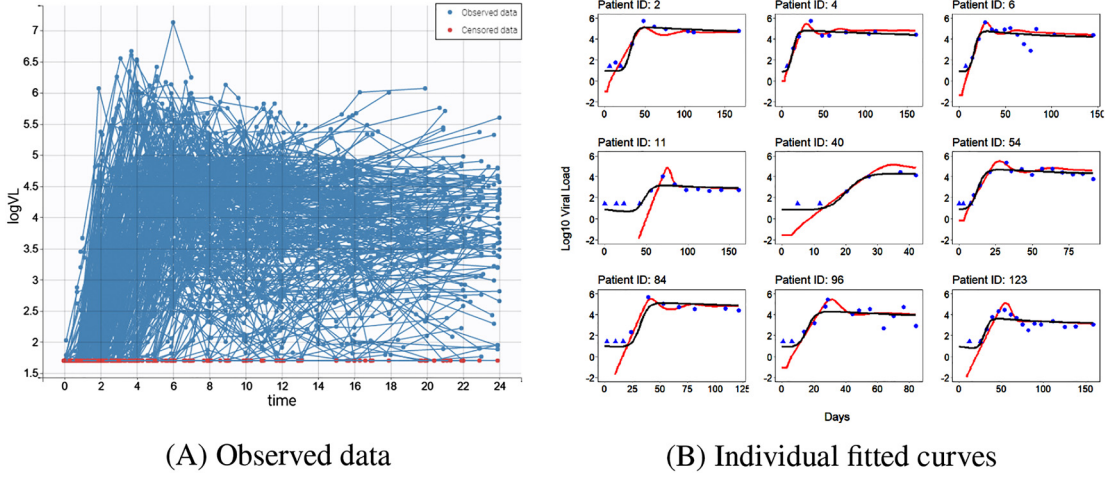


**Figure 2:** (A): Observed viral load data for 346 individuals who underwent interruption of antiretroviral therapy. (B): Model-fitted curves for nine selected individuals. The blue dots represent observed viral load ( $\log_{10}$ -transformed) values over time. The blue triangles represent viral load values that were below assay limit (i.e., <50 copies/mL) and were plotted at the assay limit. The black line represents the empirical non-linear mixed effects (NLME) model fitted curve, and the red line represents the viral dynamics model-fitted curve.

**Table 2:** Estimates of fixed-effects parameters ( $\hat{\beta}$ ) and standard deviations of the random effects parameters ( $\hat{\omega}$ ), and their standard error estimates (S.E.) from the empirical NLME and viral dynamics model.

Empirical NLME model		Viral dynamics model			
Parameters	$\hat{\beta}$ (S.E.)	$\hat{\omega}$ (S.E.)	Parameters		
$\beta_1$	3.61 (0.052)	0.75 (0.035)	$\lambda$	494.00 (6.180)	0.15 (0.009)
$\beta_2$	6.94 (0.220)	3.12 (0.169)	$\beta$	$3.72 (0.036) \times 10^{-7}$	0.05 (0.007)
$\beta_3$	2.12 (0.064)	0.67 (0.046)	$t_a$	0.03 (0.006)	2.89 (0.129)
$\beta_4$	1.72 (0.059)	0.31 (0.043)	$N_p$	$40.40 (9.68) \times 10^{-5}$	2.91 (0.168)
$\beta_5$	0.12 (0.016)	0.14 (0.014)	$p$	5.57 (0.773)	0.97 (0.128)
—	—	—	$m$	67.90 (21.000)	4.18 (0.224)

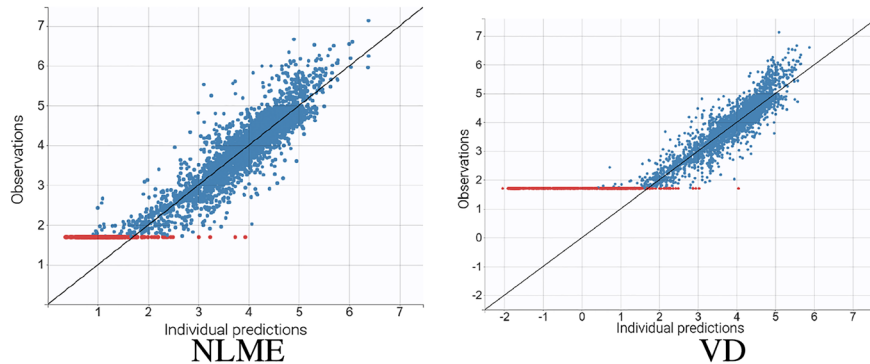
**Table 3:** Model fitting statistics for the empirical NLME and viral dynamics (VD) models.

	NLME	VD
–2 Log-likelihood	6,680.10	6,530.65
Akaike information criteria (AIC)	6,702.10	6,562.65
Bayesian information criteria (BIC)	6,744.41	6,624.19
Corrected Bayesian information criteria (BICc)	6,758.99	6,641.20

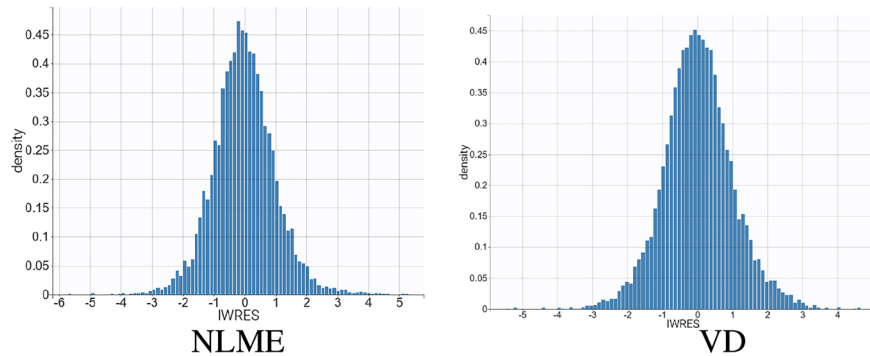
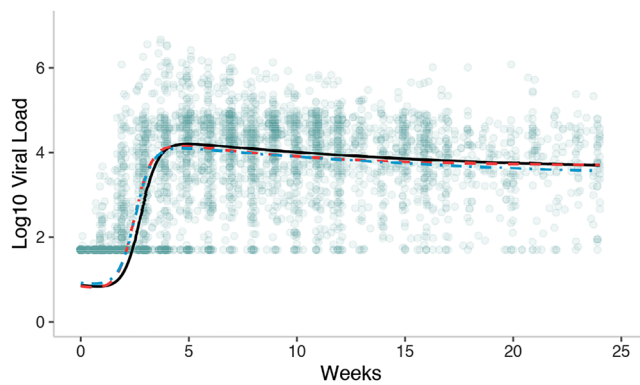
random effects associated with  $\beta_1$  and/or  $\beta_2$  in the empirical model and found that the fitted reference curves (i.e., mean prediction curves corresponding to setting random effects as 0) were very similar (Figure 3C).

Figure 4 presents a histogram of viral load set points obtained using two modeling approaches. The median set points obtained from two approaches were similar: 4.44  $\log_{10}$  copies/mL from the empirical NLME

(A) Observation vs prediction using individual parameters



(B) Distribution of the individual weighted residuals (IWRES)

(C) Reference curves when using different random effects distributions for  $\beta_1$  and  $\beta_2$  in the NLME model

**Figure 3:** Model fit analysis. (A, B) NLME: Empirical nonlinear mixed effect model. VD: viral dynamics model. IWRES are estimates of the standardized residual based on individual predictions. (C) Black solid, original model; Red dashed, random effects for  $\beta_2$  lognormal; Blue dashed dotted, random effects for  $\beta_1, \beta_2$  lognormal.

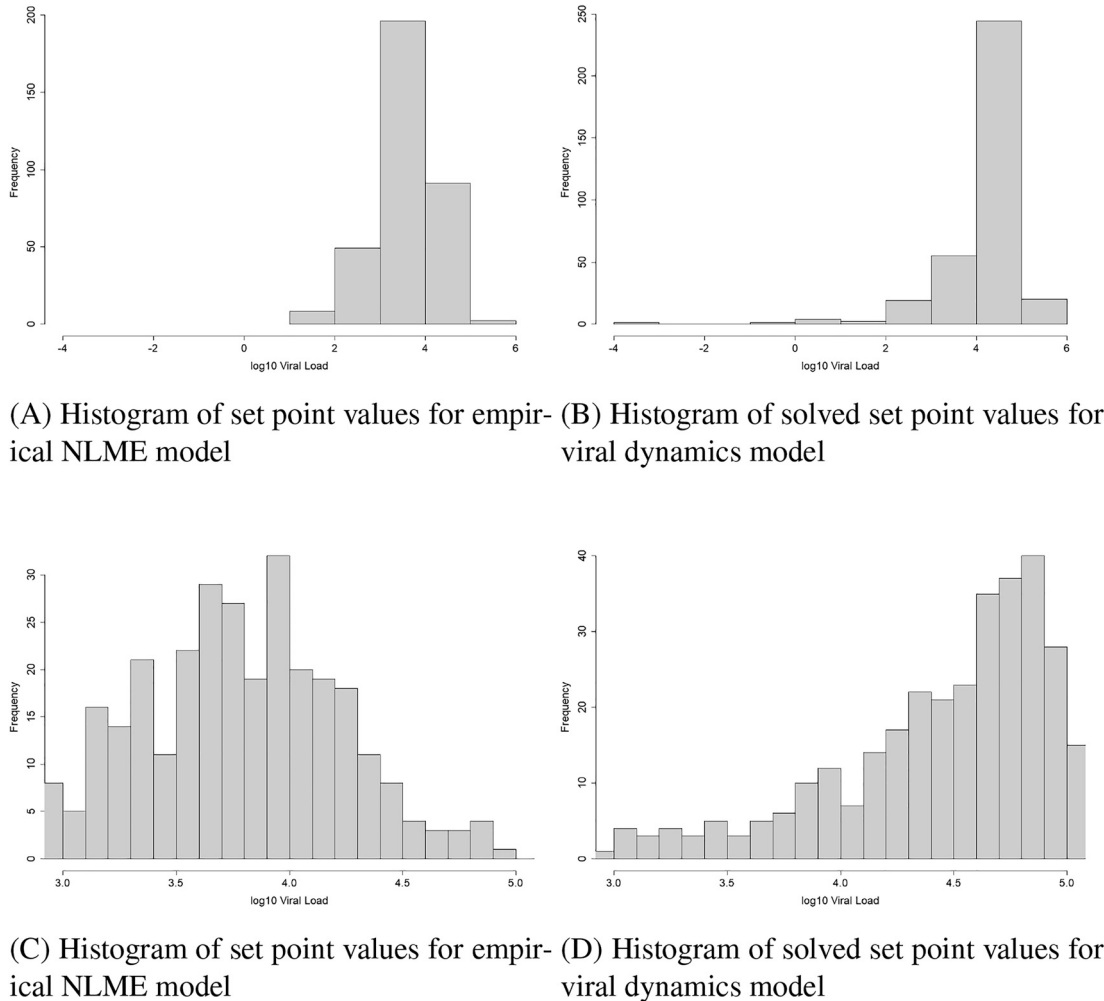


**Figure 4:** Histogram of set point values for empirical NLME model and viral dynamics model. The scale of (A) and (B) is between –4 and 6. The scale of (C) and (D) is between 3 and 5.

model and 4.59 log<sub>10</sub> copies/mL from the viral dynamics model. Viral set points obtained from the empirical model were more symmetrically distributed, reflecting the assumption that random effects were normally distributed. By contrast, the values obtained from the viral dynamics model were more skewed, with the lower tail including very low values – possibly reflecting the behavior of post-treatment controllers.

When the likelihood has several local maxima, the SAEM algorithm does not guarantee convergence to the global maximum of the likelihood. The SAEM algorithm used in Monolix makes uses of a simulated annealing variant which improves the chance of converging to the global maximum (Kirkpatrick 1984; Lavielle 2014). We performed sensitivity analyses using a range of different initial values and found that the resulting parameter estimates did not differ substantially. Results are summarized in Figures 5 and 6. In practice, we recommend careful selection of initial values by fitting simplified models, and running multiple chains and compare the corresponding likelihood values to identify a global maximum.

We used both the empirical NLME model and the viral dynamics model to assess covariate effects on delay in rebound and viral set points. The covariates we examined include: age at treatment interruption, Nadir CD4 count, the use of a NNRTI based regimen prior to ATI, infection phase at ART initiation (chronic vs. acute/recent), and ART duration. Univariate and multivariate results are presented in Tables 4 and 5 respectively.

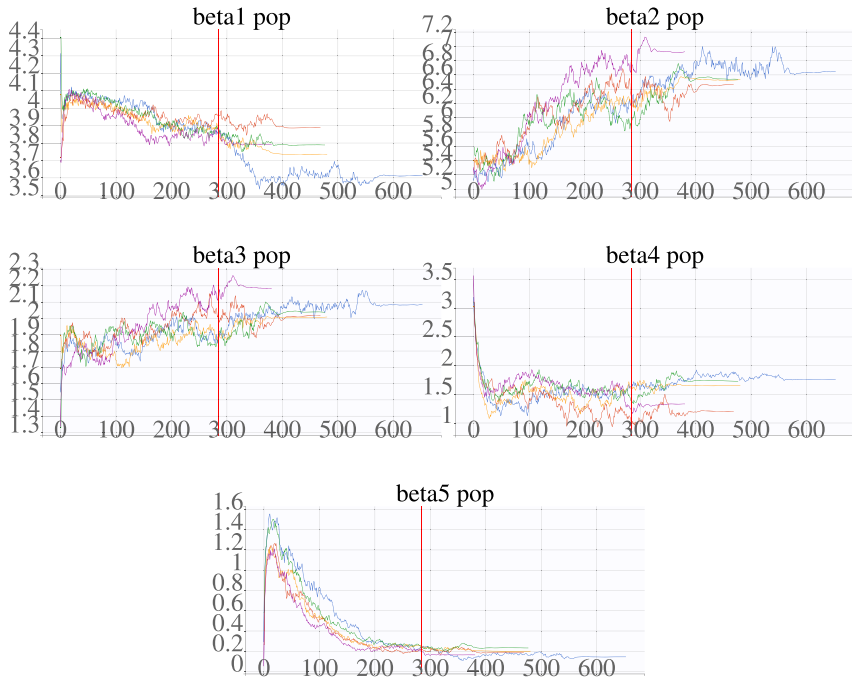


**Figure 5:** Convergence plots for empirical NLME model. The range of initial parameters:  
 $\beta_1 \in (3.65, 4.45)$ ,  
 $\beta_2 \in (4.97, 5.77)$ ,  
 $\beta_3 \in (1.25, 2.05)$ ,  
 $\beta_4 \in (2.89, 3.69)$ ,  
 $\beta_5 \in (-0.07, 0.83)$ .

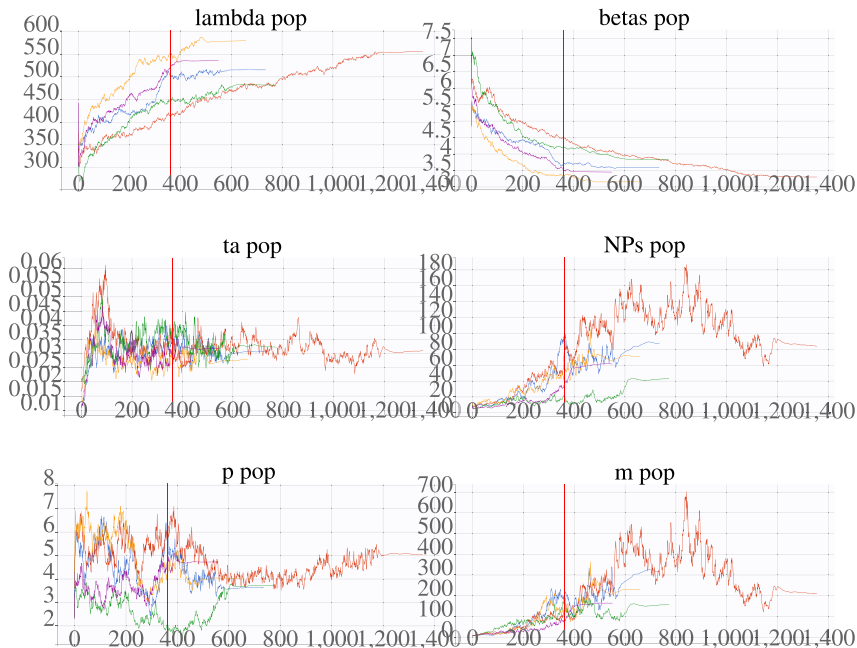


**Figure 6:** Convergence plots for viral dynamics model. The range of initial parameters:  
 $\lambda \in (300.16, 444.08)$ ,  
 $\beta \in (4.21, 7.74)$ ,  $t_a \in (0.01, 0.02)$ ,  $N_p \in (7.64, 13.33)$ ,  
 $p \in (2.50, 4.94)$ , and  $m \in (3.30, 5.27)$ .

Both models identified NNRTI-based pre-ATI regimen as a predictor for a delay in rebound. After including NNRTI-based regimen in the model, higher nadir CD4 count or older age were also seen to be associated a delay in rebound in the empirical NLME model or in the viral dynamics model respectively. Both models revealed that higher nadir CD4 cell counts and ART initiation during acute/recent phase were associated with lower viral set points.

We performed additional analyses to assess the effect of receiving immune-stimulating interventions before ATI on viral rebound trajectories. One analysis was based on fitting the models separately among

**Table 4:** Univariate covariate effects on delay in rebound and viral set points.

Delay in rebound		Empirical NLME ( $\beta_2$ )		Viral dynamics model ( $t_d$ )	
Covariates		$\widehat{\beta} (\text{S.E.})^a$	p-Value	$\widehat{\beta} (\text{S.E.})^a$	p-Value
Age at ATI		0.048 (0.022)	0.027	0.058 (0.020)	0.003
Nadir CD4 count					
>500 vs. ≤500 cells/mm <sup>3</sup>		0.613 (0.426)	0.150	0.229 (0.002)	<0.001
NNRTI-based regimen					
Yes vs. No		3.280 (0.317)	<0.001	2.750 (0.296)	<0.001
Infection phase at ART initiation					
Chronic vs. acute/recent		0.964 (0.395)	0.015	1.190 (0.024)	<0.001
Duration of ART (in years)		0.049 (0.051)	0.330	0.060 (0.045)	0.178
Viral set points		Empirical NLME ( $\beta_1$ )		Viral dynamics model	
Covariates		$\widehat{\beta} (\text{S.E.})^b$	p-Value	$\widehat{\beta} (\text{S.E.})^b$	p-Value
Age at ATI		0.026 (0.006)	<0.001	0.012 (0.007)	0.075
Nadir CD4 count					
>500 vs. ≤500 cells/mm <sup>3</sup>		-0.553 (0.105)	<0.001	-0.502 (0.116)	<0.001
NNRTI-based regimen					
Yes vs. No		0.334 (0.097)	<0.001	0.077 (0.109)	0.484
Infection phase at ART initiation					
Chronic vs. acute/recent		0.570 (0.104)	<0.001	0.371 (0.118)	0.002
Duration of ART (in years)		0.040 (0.013)	0.002	0.026 (0.015)	0.077

<sup>a</sup>The  $\beta$  coefficient represents difference in the targeted parameter ( $\beta_2$  for NLME and  $\log(t_d)$  for VD) corresponding to one unit increase in the covariate.

<sup>b</sup>The  $\beta$  coefficient represents the difference in viral set points ( $\log_{10}$ -transformed) for one unit increase in the covariate.

**Table 5:** Multivariate covariate effects on delay in rebound and viral set points.

Delay in rebound		Empirical NLME ( $\beta_2$ )		Viral dynamics model ( $t_d$ )	
Covariates		$\widehat{\beta} (\text{S.E.})^a$	p-Value	$\widehat{\beta} (\text{S.E.})^a$	p-Value
Age at ATI		—	—	0.039(0.109)	0.035
Nadir CD4 count					
>500 vs. ≤500 cells/mm <sup>3</sup>		0.865 (0.377)	0.022	—	—
NNRTI-based regimen					
Yes vs. No		3.661 (0.340)	<0.001	2.640 (0.299)	<0.001
Viral set points		Empirical NLME ( $\beta_1$ )		Viral dynamics model	
Covariates		$\widehat{\beta} (\text{S.E.})^b$	p-Value	$\widehat{\beta} (\text{S.E.})^b$	p-Value
Age at ATI		0.013 (0.005)	0.029	—	—
Nadir CD4 count					
>500 vs. ≤500 cells/mm <sup>3</sup>		-0.386 (0.104)	<0.001	-0.433 (0.120)	<0.001
Infection phase at ART initiation					
Chronic vs. acute/recent		0.367 (0.111)	<0.001	0.253 (0.121)	0.037

<sup>a</sup>The  $\beta$  coefficient represents difference in the targeted parameter ( $\beta_2$  for NLME and  $\log(t_d)$  for VD) corresponding to one unit increase in the covariate of interest, adjusting for other covariates in the model.

<sup>b</sup>The  $\beta$  coefficient represents the difference in viral set points ( $\log_{10}$ -transformed) for one unit increase in the covariate of interest, adjusting for other covariates in the model.

participants who had received immune-stimulating interventions prior to ATI and among those who had not. This analysis was done for all participants and also restricted to study A5197 because ATI set point was a primary endpoint of the study and a vaccine benefit trend, a  $0.26 \log_{10}$  copies/mL lower in set point, comparing the vaccine arm to the placebo arm was reported (Schooley et al. 2010). The resulting stratified reference curves (i.e., curves corresponding to setting random effects as 0) are presented in Figure 7. The stratified reference curves were similar when combining data across studies (Figure 7A). When limiting attention to A5197, a lower viral load set point was observed ( $3.80$  vs.  $4.44 \log_{10}$  copies/mL) – consistent with the findings in Schooley et al. (2010). A stratified analysis using the viral dynamic model also yielded a lower viral load set point for those who had received immune-stimulating interventions prior to ATI. We fit a univariate model with an indicator for treatment status added to  $\beta_1$  of the empirical model, and estimated a  $0.18 \log_{10}$  lower in the viral set point (p-value = 0.16) for the treated group.

## 4 Discussion

This paper presents model fitting results from two very different modeling approaches. The parameters of the empirical NLME model directly reflect features of the viral rebound trajectory, such as rate of rise and viral set points. This model provides direct assessment of pre-ATI predictors on these features. The dynamic model derives from a set of assumptions about the underlying within-host viral rebound dynamics: for example, latently infected cells may become reactivated to become productively infected cells, which can die or release virus to generate new infected cells. The prey/predator interactions between the virus and the immune system are captured by tracking immune cell targets as well as an antiviral immune response. The parameters (e.g., target cell replenishment rate  $\lambda$ , infection rate  $\beta$ , the latent cell reactivation rate  $a$ , precursor immune cell production rate  $m$ ) have direct biological interpretations. In general, the parameters in the two models have different interpretations: those in the empirical model represent features of the viral rebound trajectories explicitly; those in the viral dynamics model represent different aspects of viral rebound kinetics in terms of interactions of HIV viral particles and immune cells, which drive the viral rebound trajectories implicitly as characterized in Figure 1B. For example, higher target cell production rate  $\lambda$  is associated with faster rate of increase of viremia during rebound.

Although based on different sets of assumptions, both modeling approaches identified the use of a non-nucleoside reverse transcriptase inhibitor-containing regimen as being associated with delayed viral rebound. This finding is consistent with Prague et al. (2019), who fit this model to a subset of ACTG patients with very frequent viral load sampling during rebound. They allowed for a “washout” time after ART was stopped before infection could spread, and found that this time was increased by about 3 days in individuals receiving NNRTI-based ART. A similar result was found by Li et al. (2016) and Conway, Perelson, and Li (2019), who examined only the time to rebound, and found that the time was longer after interruption of an NNRTI-based regimen. The hypothesis is that the higher half-life of NNRTI drugs compared to NRTI or PI classes implies a longer time until NNRTI drug levels decay sufficiently to allow spread of reactivating infection (Usach, Melis, and Peris 2013). Because choice of ART could confound inference on viral rebound kinetics, and also lead to NNRTI resistance, treatment interruption studies now preclude use of NNRTI or other long-acting anti-retrovirals prior to ATI (Julg et al. 2019).

A major difference of our models compared to previous approaches is that we consider the full time course of rebound – as opposed to focusing only on the time to first detectable viral load which depends on frequency of measurements. We also addressed left-censoring of HIV RNA measurements in the analyses. Using both an empirical non-linear function and a viral dynamic model described by a system of differential equations, we base estimates of time until viral load exceeds a threshold on all available information. This has important statistical as well as clinical implications. From a statistical point of view, there may be predictors that are strongly associated with only particular features of viral rebound (such as set point), but not with others (such as timing). Such a scenario is consistent with current beliefs regarding HIV dynamics. Data from ACTG A5197

provided an illustration that different interventions may impact different features of viral rebound trajectory: whereas the vaccine group appeared to have a lower set point, the initial rising phases of the vaccine and placebo groups were very similar (see Figure 7B).

From a clinical point of view, some characteristics of rebound might be important for trials that conform to requirements that ATI be of short duration (e.g., timing of rebound) whereas other characteristics might be more important for assessing long-term patient outcomes (e.g., set point viral load). In addition, investigators might be interested in studying both mechanisms of drug action—for example in reducing HIV reservoirs—as well as drug effects on features of RNA rebound. The former might be based on estimation of dynamic model parameters, and the latter might focus of time to rebound or set point. The viral dynamics model attempts to model the rebound kinetics and makes more assumptions for the underlying mechanisms while the fitting of the empirical model is informed by the observed viral load values only. As such, if the assumptions hold, we would expect the viral dynamics model to make more efficient use of the data. Both models are nonlinear mixed effects models and may be sensitive to model mis-specification. Hence, it would be valuable to use both

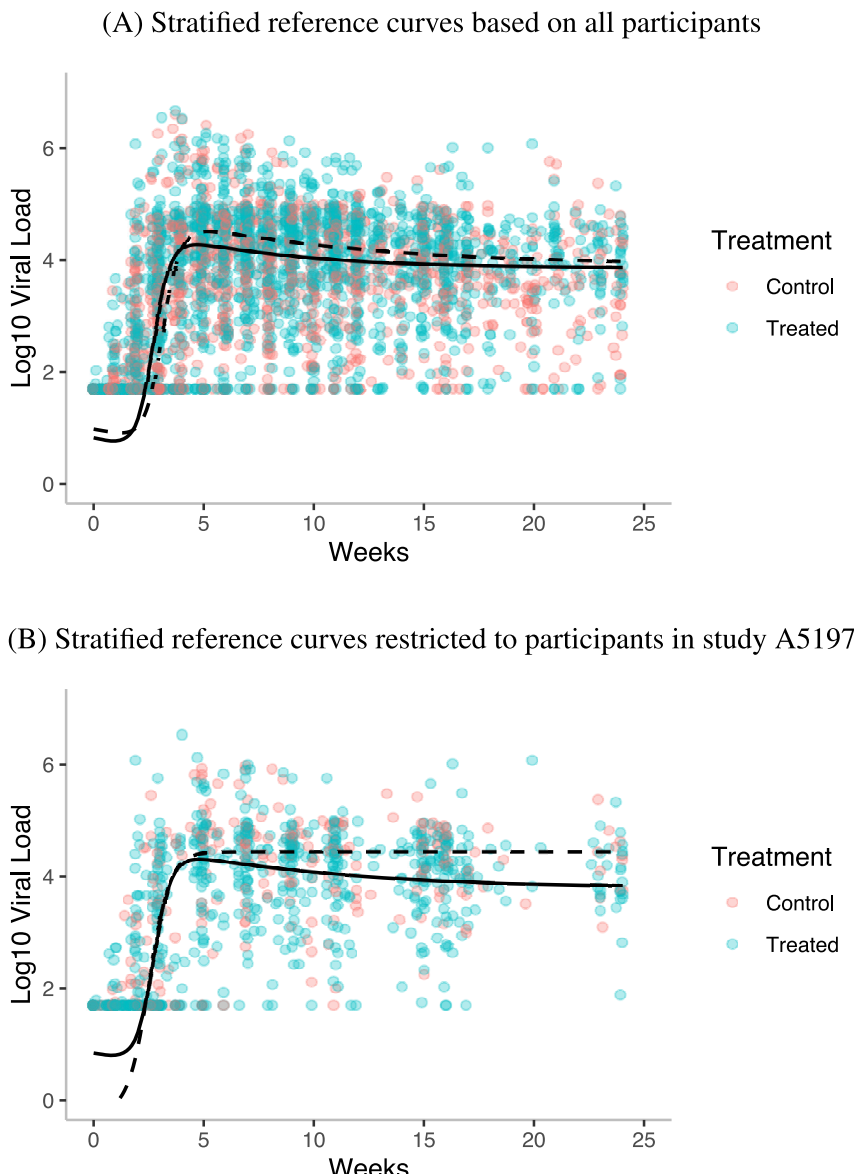


**Figure 7:** Reference curves obtained from the empirical NLME model, stratified by treatment (immune-stimulating) status. Solid: treatment group; dashed: control group.

models for investigations such as characteristics of rebound and to assess the extent to which conclusions derived from them are in agreement. Such consistency may help lend credence to results obtainable only by one type of model.

Both modeling approaches permit the assessment of pre-ATI predictors on each model parameter. The empirical model provides a means to assess the relationship between rate of rise or delay in rebound and viral set points: examining the covariance of the random effects associated with the parameters that represent these trajectory features. Future work on estimation of a flexible unstructured variance-covariance matrix for the random effects would be useful. For assessment of covariate effects on the viral set points obtained from the viral dynamics model, as the viral set point is not represented by a single parameter in the model, a two-stage approach was employed. We recognize that by ignoring the fact that viral set points are obtained as functions of multiple parameter estimates from the first stage, this two-stage approach might introduce bias into the second-stage inference (Yang et al. 2018). We note that the development of valid inference methods for such settings is needed. Our analyses focus on the assessment of covariate effects on two important features of viral rebound trajectories: delay in rebound and viral load set points. It would also be of interest to evaluate the covariate effects on each of the individual parameters in the viral dynamics model to separate out effects of covariates on each component of the underlying viral dynamics process.

In both models, normality assumptions are assumed for the random effect distributions. Testing for normality of the random effects distribution is important but difficult because the random effects are unobserved. Furthermore, lack of normality in mixed models may arise from the error terms or the unobserved random effects. For one-way error component model with balanced data, Galvao et al. (2013) proposed a test for normality based on testing for skewness and kurtosis. For imbalanced settings, Chen and Wang (2020) developed a normality test for the random effect distribution through the use of the Fleishman distribution, a flexible four-parameter distribution which accounts for the third and fourth cumulants. Verbeke and Molenberghs (2013) proposed a gradient function, a sample average of the ratios of conditional and marginal likelihood contributions for all individuals in the sample, as an exploratory diagnostic tool. Drikvandi, Verbeke, and Molenberghs (2017) further developed a formal diagnostic test based on this estimated gradient function. It would be useful to extend this test to the current setting where the observations may be censored.

The consequences of misspecifying random effects distribution have been studied in both linear mixed effects models (see for example, Butler and Louis, 1992; Verbeke and Lesaffre 1997), generalized linear mixed effects models (McCulloch and Neuhaus 2011), and nonlinear mixed effects models (Hartford and Davidian 2000; Drikvandi 2019). These investigations suggested that the inference on fixed effects is relatively robust to the violation of normality assumption for the random effects, while the inference on higher-order parameters (e.g., variance) is sensitive to the normality assumption. This is not surprising as inference for first-order quantities requires accurate estimation of second moments; while inference for second-order quantities requires accurate estimation of moments up to the fourth moments, where a normal distribution would fail to account for the skewness and kurtosis. We note that for the nonlinear mixed effects models, the consequences of misspecifying random effects distribution also depend on the use of approximate inferential methods due to the need to evaluate an intractable integral marginalizing out the random effects. Hartford and Davidian (2000) compared the first-order expansion method (Sheiner and Beal 1980) and the Laplace approximation method (Wolfinger and Lin 1997), while Drikvandi (2019) focused on the use of Gauss–Hermite quadrature. It would be useful to confirm that the general conclusion also holds when a SAEM algorithm is employed as in the current paper.

Our analyses were based only on repeated viral load measurements. It would be of interest to investigate whether joint modeling with other measures such as CD4 cell counts, which decline after ART interruption (Li et al. 2016), improves model fit. The dynamic model is intended to represent the mechanism of interaction between virus and immune system; hence, it describes the dynamics of main HIV target immune cells – CD4+ T cells. Incorporating CD4 cell counts may improve the identifiability of the model parameters. The pre-ATI predictors we evaluated reflect values at a single time point (e.g., age at the start of treatment interruption), or provide summaries over history (e.g., nadir CD4 count). Future work might profitably focus on investigation of the effect of longitudinal history profiles on features of viral rebound.

**Acknowledgments:** We thank the participants, staff, and principal investigators of the ACTG studies 371, A5024, A5068, A5130, A5187, and A5197.

**Research funding:** We gratefully acknowledge grants from National Institute of Allergy and Infectious Diseases P01 AI131385, P01 AI131365, R37 AI051164, and R01 AI136947, UM1 AI068634, UM1 AI068636, and an amfAR Impact Grant 109856-65-RGRL from the Foundation for AIDS Research, and the Inria Associate team, project DYNAMHIC.

**Author contributions:** All authors have accepted responsibility for the entire content of this manuscript and approved its submission.

**Competing interests:** Authors state no conflict of interest.

## References

- Bellu, G., M. P. Saccomani, S. Audoly, and L. D'Angiò. 2007. "Daisy: A New Software Tool to Test Global Identifiability of Biological and Physiological Systems." *Computer Methods and Programs in Biomedicine* 88: 52–61.
- Borducchi, E. N., J. Liu, J. P. Nkolola, A. M. Cadena, W.-H. Yu, S. Fischinger, T. Broge, P. Abbink, N. B. Mercado, A. Chandrashekhar, D. Jetton, L. Peter, K. McMahan, E. T. Moseley, E. Bekerman, J. Hesselgesser, W. Li, M. G. Lewis, G. Alter, R. Gelezunas, and D. H. Barouch. 2018. "Antibody and TLR7 Agonist Delay Viral Rebound in SHIV-Infected Monkeys." *Nature* 563: 360–4.
- Brown, E. R., J. G. Ibrahim, and V. DeGruttola. 2005. "A Flexible B-Spline Model for Multiple Longitudinal Biomarkers and Survival." *Biometrics* 61: 64–73.
- Butler, S. M., and T. A. Louis. 1992. "Random Effects Models with Non-parametric Priors." *Statistics in Medicine* 11: 1981–2000.
- Castro, M., and R. J. de Boer. 2020. "Testing Structural Identifiability by a Simple Scaling Method." *bioRxiv*. <https://doi.org/10.1101/2020.02.04.933630>.
- Chen, H. Y., M. Di Mascio, A. S. Perelson, D. D. Ho, and L. Zhang. 2007. "Determination of Virus Burst Size In Vivo Using a Single-Cycle SIV in Rhesus Macaques." *Proceedings of the National Academy of Sciences* 104: 19079–84.
- Chen, T., and R. Wang. 2020. "Inference for Variance Components in Linear Models with Flexible Random Effect and Error Distributions." *Statistical Methods in Medical Research*. forthcoming. <https://doi.org/10.1177/0962280220933909>.
- Comets, E., A. Lavenu, and M. Lavielle. 2011. "SAEMIX, an R Version of the SAEM Algorithm." *20th Meeting of the Population Approach Group in Europe, Athens, Greece. Abstr, volume 2173*.
- Conway, J. M., and A. S. Perelson. 2015. "Post-treatment Control of HIV Infection." *Proceedings of the National Academy of Sciences* 112: 5467–72.
- Conway, J. M., A. S. Perelson, and J. Z. Li. 2019. "Predictions of Time to HIV Viral Rebound Following Art Suspension that Incorporate Personal Biomarkers." *PLoS Computational Biology* 15: e1007229.
- Dagne, G. A., 2016. "Bayesian Segmental Growth Mixture Tobit Models with Skew Distributions." *Computational Statistics* 31: 121–37.
- Drikvandi, R., 2019. "Nonlinear Mixed-Effects Models with Misspecified Random-Effects Distribution." *Pharmaceutical Statistics* 19: 187–201.
- Drikvandi, R., G. Verbeke, and G. Molenberghs. 2017. "Diagnosing Misspecification of the Random-Effects Distribution in Mixed Models." *Biometrics* 73: 63–71.
- Drylewicz, J., D. Commenges, and R. Thiebaut. 2012. "Maximum A Posteriori Estimation in Dynamical Models of Primary HIV Infection." *Statistical Communications in Infectious Diseases* 4. <https://doi.org/10.1515/1948-4690.1040>.
- Dybul, M., A. S. Fauci, J. G. Bartlett, J. E. Kaplan, and A. K. Pau. 2002. "Guidelines for Using Antiretroviral Agents Among HIV-Infected Adults and Adolescents: The Panel on Clinical Practices for Treatment of HIV." *Annals of Internal Medicine* 137: 381–433.
- Fitzgerald, A. P., V. G. DeGruttola, and F. Vaida. 2002. "Modelling HIV Viral Rebound Using Non-linear Mixed Effects Models." *Statistics in Medicine* 21: 2093–108.
- Galvao, A. F., G. Montes-Rojas, W. Sosa-Escudero, and L. Wang. 2013. "Tests for Skewness and Kurtosis in the One-Way Error Component Model." *Journal of Multivariate Analysis* 122: 35–52.
- Gandhi, R. T., D. O'Neill, R. J. Bosch, E. S. Chan, R. P. Bucy, J. Shopis, L. Baglyos, E. Adams, L. Fox, L. Purdue, A. Marshak, T. Flynn, R. Masih, B. Schock, D. Mildvan, S. J. Schlesinger, M. A. Marovich, N. Bhardwaj, and J. M. Jacobson. 2009. "A Randomized Therapeutic Vaccine Trial of Canarypox-HIV-Pulsed Dendritic Cells vs. Canarypox-HIV Alone in HIV-1-Infected Patients on Antiretroviral Therapy." *Vaccine* 27: 6088–94.
- Garay, A. M., L. M. Castro, J. Leskow, and V. H. Lachos. 2017. "Censored Linear Regression Models for Irregularly Observed Longitudinal Data Using the Multivariate-t Distribution." *Statistical Methods in Medical Research* 26: 542–66.
- Guedj, J., R. Thiébaut, and D. Commenges. 2007. "Maximum Likelihood Estimation in Dynamical Models of HIV." *Biometrics* 63: 1198–206.

- Hartford, A., and M. Davidian. 2000. "Consequences of Misspecifying Assumptions in Nonlinear Mixed Effects Models." *Computational Statistics & Data Analysis* 34: 139–64.
- Hill, A. L., D. I. Rosenbloom, E. Goldstein, E. Hanhauser, D. R. Kuritzkes, R. F. Siliciano, and T. J. Henrich. 2016. "Real-time Predictions of Reservoir Size and Rebound Time during Antiretroviral Therapy Interruption Trials for HIV." *PLoS Pathogens* 12. <https://doi.org/10.1371/journal.ppat.1005535>.
- Ho, D. D., A. U. Neumann, A. S. Perelson, W. Chen, J. M. Leonard, and M. Markowitz. 1995. "Rapid Turnover of Plasma Virions and CD4 Lymphocytes in HIV-1 Infection." *Nature* 373: 123–6.
- Huang, Y., and G. Dagne. 2010. "Skew-normal Bayesian Nonlinear Mixed-Effects Models with Application to AIDS Studies." *Statistics in Medicine* 29: 2384–98.
- Huang, Y., and G. Dagne. 2012. "Bayesian Semiparametric Nonlinear Mixed-Effects Joint Models for Data with Skewness, Missing Responses, and Measurement Errors in Covariates." *Biometrics* 68: 943–53.
- Huang, Y., D. Liu, and H. Wu. 2006. "Hierarchical Bayesian Methods for Estimation of Parameters in a Longitudinal HIV Dynamic System." *Biometrics* 62: 413–23.
- Jacobson, J. M., R. Pat Bucy, J. Spritzler, M. S. Saag, J. J. Eron, Jr., R. W. Coombs, R. Wang, L. Fox, V. A. Johnson, S. Cu-Uvin, S. E. Cohn, D. Mildvan, D. O'Neill, J. Janik, L. Purdue, D. K. O'Connor, C. D. Vita, and I. Frank. 2006. "Evidence that Intermittent Structured Treatment Interruption, but Not Immunization with ALVAC-HIV vCP1452, Promotes Host Control of HIV Replication: The Results of AIDS Clinical Trials Group 5068." *The Journal of Infectious Diseases* 194: 623–32.
- Julg, B., L. Dee, J. Ananworanich, D. H. Barouch, K. Bar, M. Caskey, D. J. Colby, L. Dawson, K. L. Dong, K. Dubé, J. Eron, J. Frater, R. T. Gandhi, R. Geleziunas, P. Goulder, G. J. Hanna, R. Johnston, D. Kuritzkes, J. Z. Li, U. Likhitwonnawut, J. van Lunzen, J. Martinez-Picado, V. Miller, L. J. Montaner, D. F. Nixon, D. Palm, G. Pantaleo, H. Peay, D. Persaud, J. Salzwedel, K. Salzwedel, T. Schacker, V. Sheikh, O. S. Søgaard, S. Spudich, K. Stephenson, J. Sugarman, J. Taylor, P. Tebas, C. T. Tiemessen, R. Tressler, C. D. Weiss, L. Zheng, M. L. Robb, N. L. Michael, J. W. Mellors, S. G. Deeks, and B. D. Walker. 2019. "Recommendations for Analytical Antiretroviral Treatment Interruptions in HIV Research Trials—Report of a Consensus Meeting." *The Lancet HIV* 6: e259–68.
- Karlsson, J., M. Anguelova, and M. Jirstrand. 2012. "An Efficient Method for Structural Identifiability Analysis of Large Dynamic Systems." *IFAC Proceedings Volumes* 45: 941–6.
- Kilby, J. M., R. P. Bucy, D. Mildvan, M. Fischl, J. Santana-Bagur, J. Lennox, C. Pilcher, A. Zolopa, J. Lawrence, R. B. Pollard, R. E. Habib, D. Sahner, L. Fox, E. Aga, R. J. Bosch, and R. Mitsuyasu. 2006. "A Randomized, Partially Blinded Phase 2 Trial of Antiretroviral Therapy, HIV-specific Immunizations, and Interleukin-2 Cycles to Promote Efficient Control of Viral Replication (ACTG A5024)." *The Journal of Infectious Diseases* 194: 1672–6.
- Kirkpatrick, S., 1984. "Optimization by Simulated Annealing: Quantitative Studies." *Journal of Statistical Physics* 34: 975–86.
- Lachos, V. H., D. Bandyopadhyay, and D. K. Dey. 2011. "Linear and Nonlinear Mixed-Effects Models for Censored HIV Viral Loads Using Normal/independent Distributions." *Biometrics* 67: 1594–604.
- Lachos, V. H., M.-H. Chen, C. A. Abanto-Valle, and C. L. Azevedo. 2015. "Quantile Regression for Censored Mixed-Effects Models with Applications to Hiv Studies." *Statistics and Its Interface* 8: 203.
- Lavielle, M., 2014. *Mixed Effects Models for the Population Approach: Models, Tasks, Methods and Tools*. Boca Raton, FL: CRC Press.
- Li, J. Z., B. Etemad, H. Ahmed, E. Aga, R. J. Bosch, J. W. Mellors, D. R. Kuritzkes, M. M. Lederman, M. Para, and R. T. Gandhi. 2016. "The Size of the Expressed HIV Reservoir Predicts Timing of Viral Rebound after Treatment Interruption," *AIDS (London, England)* 30: 343.
- Liang, H., and Y. Xiao. 2006. "Penalized Splines for Longitudinal Data with an Application in Aids Studies." *Journal of Modern Applied Statistical Methods* 5: 12.
- Liu, B., L. Wang, Y. Nie, and J. Cao. 2019. "Bayesian Inference of Mixed-Effects Ordinary Differential Equations Models Using Heavy-Tailed Distributions." *Computational Statistics & Data Analysis* 137: 233–46.
- Markowitz, M., M. Louie, A. Hurley, E. Sun, M. Di Mascio, A. S. Perelson, and D. D. Ho. 2003. "A Novel Antiviral Intervention Results in More Accurate Assessment of Human Immunodeficiency Virus Type 1 Replication Dynamics and t-cell Decay In Vivo." *Journal of Virology* 77: 5037–8.
- Matos, L. A., M. O. Prates, M.-H. Chen, and V. H. Lachos. 2013. "Likelihood-based Inference for Mixed-Effects Models with Censored Response Using the Multivariate-t Distribution." *Statistica Sinica*: 1323–45. <https://doi.org/10.5705/ss.2012.043>.
- McCulloch, C. E., and J. M. Neuhaus. 2011. "Misspecifying the Shape of a Random Effects Distribution: Why Getting it Wrong May Not Matter." *Statistical Science*: 388–402. <https://doi.org/10.1214/11-sts361>.
- Mellors, J. W., A. Munoz, J. V. Giorgi, J. B. Margolick, C. J. Tassoni, P. Gupta, L. A. Kingsley, J. A. Todd, A. J. Saah, R. Detels, and J.P. Phair. 1997. "Plasma Viral Load and CD4+ Lymphocytes as Prognostic Markers of HIV-1 Infection." *Annals of Internal Medicine* 126: 946–54.
- Moulton, L. H., F. C. Curriero, and P. F. Barroso. 2002. "Mixture Models for Quantitative HIV RNA Data." *Statistical Methods in Medical Research* 11: 317–25.
- Nowak, M., and R. May. 2000. *Virus Dynamics: Mathematical Principles of Immunology and Virology*. Oxford: University of Oxford.
- Perelson, A. S., P. Essunger, Y. Cao, M. Vesanen, A. Hurley, K. Saksela, M. Markowitz, and D. D. Ho. 1997. "Decay Characteristics of Hiv-1-Infected Compartments during Combination Therapy." *Nature* 387: 188–91.
- Perelson, A. S., and R. M. Ribeiro. 2013. "Modeling the Within-Host Dynamics of Hiv Infection." *BMC Biology* 11: 96.

- Pinkevych, M., D. Cromer, M. Tolstrup, A. J. Grimm, D. A. Cooper, S. R. Lewin, O. S. Søgaard, T. A. Rasmussen, S. J. Kent, A. D. Kelleher, and M. P. Davenport. 2015. "HIV Reactivation from Latency after Treatment Interruption Occurs on Average Every 5-8 Days—Implications for HIV Remission." *PLoS Pathogens* 11. <https://doi.org/10.1371/journal.ppat.1005000>.
- Prague, M., D. Commenges, J. Drylewicz, and R. Thiébaut. 2012. "Treatment Monitoring of HIV-Infected Patients Based on Mechanistic Models." *Biometrics* 68: 902–11.
- Prague, M., D. Commenges, J. Guedj, J. Drylewicz, and R. Thiébaut. 2013. "NIMROD: A Program for Inference via a Normal Approximation of the Posterior in Models with Random Effects Based on Ordinary Differential Equations." *Computer Methods and Programs in Biomedicine* 111: 447–58.
- Prague, M., J. M. Gerold, I. Balelli, C. Pasin, J. Z. Li, D. H. Barouch, J. B. Whitney, and A. L. Hill. 2019. "Viral Rebound Kinetics Following Single and Combination Immunotherapy for HIV/SIV." *BioRxiv*: 700401. <https://doi.org/10.1101/700401>.
- Putter, H., S. Heisterkamp, J. Lange, and F. De Wolf. 2002. "A Bayesian Approach to Parameter Estimation in HIV Dynamical Models." *Statistics in Medicine* 21: 2199–214.
- Ramratnam, B., S. Bonhoeffer, J. Binley, A. Hurley, L. Zhang, J. E. Mittler, M. Markowitz, J. P. Moore, A. S. Perelson, and D. D. Ho. 1999. "Rapid Production and Clearance of HIV-1 and Hepatitis C Virus Assessed by Large Volume Plasma Apheresis." *The Lancet* 354: 1782–5.
- Rong, L., and A. S. Perelson. 2009. "Modeling Latently Infected Cell Activation: Viral and Latent Reservoir Persistence, and Viral Blips in HIV-Infected Patients on Potent Therapy." *PLoS Computational Biology* 5. <https://doi.org/10.1371/journal.pcbi.1000533>.
- Rosenberg, E. S., B. S. Graham, E. S. Chan, R. J. Bosch, V. Stocker, J. Maenza, M. Markowitz, S. Little, P. E. Sax, A. C. Collier, G. Nabel, S. Saïndon, T. Flynn, D. Kuritzkes, and D. H. Barouch. 2010. "Safety and Immunogenicity of Therapeutic DNA Vaccination in Individuals Treated with Antiretroviral Therapy during Acute/early HIV-1 Infection." *PLoS One* 5: e10555.
- Samson, A., M. Lavielle, and F. Mentré. 2006. "Extension of the SAEM Algorithm to Left-Censored Data in Nonlinear Mixed-Effects Model: Application to HIV Dynamics Model." *Computational Statistics & Data Analysis* 51: 1562–74.
- Schooley, R. T., J. Spritzler, H. Wang, M. M. Lederman, D. Havlir, D. R. Kuritzkes, R. Pollard, C. Battaglia, M. Robertson, D. Mehrotra, D. Casimiro, K. Cox, and B. Schock. 2010. "AIDS Clinical Trials Group 5197: A Placebo-Controlled Trial of Immunization of HIV-1-Infected Persons with a Replication-Deficient Adenovirus Type 5 Vaccine Expressing the HIV-1 Core Protein." *The Journal of Infectious Diseases* 202: 705–16.
- Schwartz, E. J., K. R. Biggs, C. Bailes, K. A. Ferolito, and N. K. Vaidya. 2016. "HIV Dynamics with Immune Responses: Perspectives from Mathematical Modeling." *Current Clinical Microbiology Reports* 3: 216–24.
- Sheiner, L. B., and S. L. Beal. 1980. "Evaluation of Methods for Estimating Population Pharmacokinetic Parameters. I. Michaelis-Menten Model: Routine Clinical Pharmacokinetic Data." *Journal of Pharmacokinetics and Biopharmaceutics* 8: 553–71.
- Thiébaut, R., H. Jacqmin-Gadda, A. Babiker, D. Commenges, and C. Collaboration. 2005. "Joint Modelling of Bivariate Longitudinal Data with Informative Dropout and Left-Censoring, with Application to the Evolution of CD4+ Cell Count and HIV RNA Viral Load in Response to Treatment of HIV Infection." *Statistics in Medicine* 24: 65–82.
- Usach, I., V. Melis, and J.-E. Peris. 2013. "Non-nucleoside Reverse Transcriptase Inhibitors: A Review on Pharmacokinetics, Pharmacodynamics, Safety and Tolerability." *Journal of the International AIDS Society* 16: 18567.
- Vaida, F., A. P. Fitzgerald, and V. DeGruttola. 2007. "Efficient Hybrid EM for Linear and Nonlinear Mixed Effects Models with Censored Response." *Computational Statistics & Data Analysis* 51: 5718–30.
- Vaida, F., and L. Liu. 2009. "Fast Implementation for Normal Mixed Effects Models with Censored Response." *Journal of Computational & Graphical Statistics* 18: 797–817.
- Vanhamel, J., A. Bruggemans, and Z. Debyser. 2019. "Establishment of Latent HIV-1 Reservoirs: What Do We Really Know?" *Journal of Virus Eradication* 5: 3.
- Verbeke, G., and E. Lesaffre. 1997. "The Effect of Misspecifying the Random-Effects Distribution in Linear Mixed Models for Longitudinal Data." *Computational Statistics & Data Analysis* 23: 541–56.
- Verbeke, G., and G. Molenberghs. 2013. "The Gradient Function as an Exploratory Goodness-of-Fit Assessment of the Random-Effects Distribution in Mixed Models." *Biostatistics* 14: 477–90.
- Volberding, P., L. Demeter, R. J. Bosch, E. Aga, C. Pettinelli, M. Hirsch, M. Vogler, A. Martinez, S. Little, and E. Connick. 2009. "Antiretroviral Therapy in Acute and Recent HIV Infection: A Prospective Multicenter Stratified Trial of Intentionally Interrupted Treatment." *AIDS (London, England)* 23: 1987.
- Wang, J., J. Pang, T. Kuniya, and Y. Enatsu. 2014. "Global Threshold Dynamics in a Five-Dimensional Virus Model with Cell-Mediated, Humoral Immune Responses and Distributed Delays." *Applied Mathematics and Computation* 241: 298–316.
- Wang, R., A. Bing, C. Wang, Y. Hu, R. J. Bosch, and V. DeGruttola. 2020. "A Flexible Nonlinear Mixed Effects Model for HIV Viral Load Rebound after Treatment Interruption." *Statistics in Medicine* 39: 2051–66.
- Wei, X., S. K. Ghosh, M. E. Taylor, V. A. Johnson, E. A. Emini, P. Deutsch, J. D. Lifson, S. Bonhoeffer, M. A. Nowak, B. H. Hahn, M. S. Saag, and G. M. Shaw. 1995. "Viral Dynamics in Human Immunodeficiency Virus Type 1 Infection." *Nature* 373: 117–22.
- Wolfinger, R. D., and X. Lin. 1997. "Two Taylor-Series Approximation Methods for Nonlinear Mixed Models." *Computational Statistics & Data Analysis* 25: 465–90.
- Wu, H., 2005. "Statistical Methods for HIV Dynamic Studies in AIDS Clinical Trials." *Statistical Methods in Medical Research* 14: 171–92.

- Wu, H., and A. A. Ding. 1999. "Population HIV-1 Dynamics In Vivo: Applicable Models and Inferential Tools for Virological Data from Aids Clinical Trials." *Biometrics* 55: 410–8.
- Wu, H., and J.-T. Zhang. 2002. "The Study of Long-Term Hiv Dynamics Using Semi-parametric Non-linear Mixed-Effects Models." *Statistics in Medicine* 21: 3655–75.
- Wu, L., 2009. *Mixed Effects Models for Complex Data*. Boca Raton, FL: Chapman and Hall/CRC.
- Yang, M., G. Adomavicius, G. Burtch, and Y. Ren. 2018. "Mind the Gap: Accounting for Measurement Error and Misclassification in Variables Generated via Data Mining." *Information Systems Research* 29: 4–24.
- Zhao, L., T. Chen, V. Novitsky, and R. Wang. 2020. "Joint Penalized Spline Modeling of Multivariate Longitudinal Data, with Application to HIV-1 RNA Load Levels and CD4 Cell Counts." *Biometrics*. forthcoming. <https://doi.org/10.1111/biom.13339>.